IRIS AperTO

UNIVERSITÀ DEGLI STUDI DI TORINO

AperTO - Archivio Istituzionale Open Access dell'Università di Torino

Size resolved metal distribution in the PM matter of the city of Turin (Italy)

This is the author's manuscript

Original Citation:

Availability:

This version is available http://hdl.handle.net/2318/1622917 since 2020-07-05T08:53:17Z

Published version:

DOI:10.1016/j.chemosphere.2015.12.089

Terms of use:

Open Access

Anyone can freely access the full text of works made available as "Open Access". Works made available under a Creative Commons license can be used according to the terms and conditions of said license. Use of all other works requires consent of the right holder (author or publisher) if not exempted from copyright protection by the applicable law.

(Article begins on next page)

04 June 2023

IRIS AperTO

UNIVERSITÀ DEGLI STUDI DI TORINO

This Accepted Author Manuscript (AAM) is copyrighted and published by Elsevier. It is posted here by agreement between Elsevier and the University of Turin. Changes resulting from the publishing process - such as editing, corrections, structural formatting, and other quality control mechanisms - may not be reflected in this version of the text. The definitive version of the text was subsequently published in CHEMOSPHERE, 147, 2016, 10.1016/j.chemosphere.2015.12.089.

You may download, copy and otherwise use the AAM for non-commercial purposes provided that your license is limited by the following restrictions:

(1) You may use this AAM for non-commercial purposes only under the terms of the CC-BY-NC-ND license.

(2) The integrity of the work and identification of the author, copyright owner, and publisher must be preserved in any copy.

(3) You must attribute this AAM in the following format: Creative Commons BY-NC-ND license (http://creativecommons.org/licenses/by-nc-nd/4.0/deed.en), 10.1016/j.chemosphere.2015.12.089

The publisher's version is available at:
http://linkinghub.elsevier.com/retrieve/pii/S0045653515305439

When citing, please refer to the published version.

Link to this full text:
http://hdl.handle.net/

This full text was downloaded from iris - AperTO: https://iris.unito.it/

iris - AperTO

University of Turin's Institutional Research Information System and Open Access Institutional Repository

Size resolved metal distribution in the PM matter of the city of Turin (Italy)

Mery Malandrino[1], Marco Casazza[2], Ornella Abollino[1], Claudio Minero[1], Valter Maurino[1*]

[1] Università degli Studi di Torino, Dipartimento di Chimica, Via P. Giuria 5, 10125, Torino, Italy

[2] University 'Parthenope' of Napoli, Department of Science and Technologies, Centro Direzionale, Isola C4, 80143, Napoli, Italy

*Corresponding Authors

MM: E-mail: mery.malandrino@unito.it, Tel +390116705249, Fax +390116707615

VM: E-mail: valter.maurino@unito.it, Tel. +390116705218; Fax: +390116707615.

Abstract

A work on the characterization of the air quality in the city of Turin was carried out in different sampling periods, reflecting late summer and winter conditions, including a snow episode during the early 2012 european cold wave.

The concentrations of 16 elements in eight size fractions of the aerosol were determined using inductively coupled plasma-mass spectrometry. The collection was carried out with a Andersen MkII cascade impactor.

The size distribution of elements allowed the identification of three main behavioural types: (a) elements associated with coarse particles (Cd, Cr, Cu, Fe, Mn, Mo, Pt and Sn); (b) elements found within fine particles (As, Co, Pb and V) and (c) elements spread throughout the entire size range (Ni, Pd, Rh and Zn).

Principal Component Analysis allowed to examine the relationships between the inorganic elements and to infer about their origin. Chemometric investigation and assessment of similarity in the distribution led to similar conclusions on the sources.

The concentration of gaseous trace pollutants (O_3, NO_x and VOCs) was determined. The concentrations of these pollutants are scarcely correlated with the metal contents of all the size classes of the PM. The differences found in the O_3, NO_2 and VOCs levels of the two winter campaigns due to the high photochemical reactivity in the period after the snow episode, do not reflect in differences in the metals distribution in the PM. Since PM metals, NO_x and VOC have common sources, this behaviour is due to relevant differences in the transformation and deposition processes.

Keywords

PM_{10}, BTEX, Ozone, Urban air quality, size distribution of elements, principal component analysis

Introduction

Air pollution represents one of the greatest concerns of urban environments. In the last decades great attention was paid to Particulate Matter (PM), due to the correlation between fine PM exposure and adverse health effects. The health burden associated to PM air pollution is one of the main environmental health concerns raised by World Health Organization (WHO, 2006). The European Environmental Agency indicates that, with respect to the PM_{10} and $PM_{2.5}$ thresholds and daily limit values, the Po Valley is one of the most critical areas in Europe (EEA, 2013).

Epidemiological and experimental studies have shown that particulate air pollution may induce and aggravate respiratory and cardiovascular diseases. Significant correlations between exposure to ambient air particles and increased morbidity and mortality have been demonstrated (Donaldson et al., 2002, Englert, 2004; Katsouyanni et al., 2001; Krewski and Rainham, 2007). Most of the available studies do not attribute the observed health effects to a particular characteristic of PM. Moreover, the exact physiochemical mechanism by which PM produces adverse effects is still unknown; one hypothesis implicates the oxidative potential of the particles or specific components. In particular, epidemiological studies have found this correlation for fine particle metrics, such as $PM_{2.5}$ (Lall et al., 2005). The pro-inflammatory effect of urban fine and ultrafine PM on human bronchial epithelial cells resulted to be concentration dependent (Ramgolan et al., 2008, Baulig et al, 2009). Short term effects of the fine PM have also been found on daily mortality due to diseases of the cardiocirculatory system (Maté et al., 2010).

PM is a complex and heterogeneous mixture, whose composition (particle size distribution and chemical characteristics) changes with time and space and depends on emissions from various sources, atmospheric chemistry and weather conditions. The coarse fraction (2.5-10 μm) comes predominantly from natural sources (geological material, such as fugitive and resuspended dust, and biological material, such as pollen and endotoxins), and its composition changes depending on the geology of the site. The fine fraction (0.1-2.5 μm) is dominated by anthropogenic emissions: a mixture of carbon particles from combustion processes and secondary particles produced by photochemical reactions in the atmosphere (sulphate, nitrate, ammonium). The carbonaceous fraction consists of aggregates of organic and elemental carbon on which transition metals, organic compounds and biological constituents are adsorbed. Penetration in the respiratory system is strictly correlated with the aerodynamic radius. Thus, so concerning the adverse health effects, the

distribution of toxic elements and compounds among the various size fractions of the PM is also of primary relevance.

Elements are released to the atmosphere from both anthropogenic and natural sources. Anthropogenic sources include fossil fuel combustion, industrial metallurgical processes, vehicle emission and waste incinerations. Natural sources include a variety of processes acting on crustal minerals, such as volcanism, erosion and surface winds, as well as from forest fires and the oceans.

Other than the effects on public health, the knowledge of the size distribution and size dependent chemical speciation is also important in identifying the sources and transformation processes during atmospheric transport. Indeed, different sources emit airborne PM with different size distribution, which are deposited at different rates. Particles with diameter in the range of 0.1 – 1.0 μm (accumulation mode) deposit slowly and can be transported far from emission sources with effects on remote areas (Allen et al., 2001). Instead, coarse particles (aerodynamic diameter > 2.7 μm) are usually emitted from local sources.

In general, as reported above, coarse particles mainly come from road dust re-suspensions, abrasion processes, crustal erosion and sea salts, whereas fine mode particles have been found to mainly derive from anthropogenic sources (combustion processes, high-temperature industrial activities, automotive traffic, etc.) (Handler et al., 2008). Therefore, source apportionment and toxicological information are enhanced by detailed knowledge of the size distribution of aerosol and of its chemical composition.

The size distribution of elements within atmospheric particles has been studied over cities around the world and a bimodal distribution of atmospheric particulates has been usually reported, e.g. in Beijing, China (Duan et al., 2012), New York, USA (Song and Gao, 2011), Kanazawa, Japan (Wang et al., 2006), San Roque, Spain (Sánchez de la Campa et al., 2011), Venice, Italy (Toscano et al., 2011, Masiol et al., 2015) and Thessaloniki, Greece (Samara et al. 2006).

Concerning the situation in Turin, Italy, time series of the size-fractioned PM_{10} mass concentration were registered. An overview of these was recently published (Casazza et al., 2013), considering winter data of years 1980, 2000 and 2011. These three years, as reported in the paper, can be associated to a known variation of sources characteristics, due to the introduction of new regulations and interventions aimed at air pollution mitigation. In particular, the first data (year 1980) are representative of the situation before the introduction of a stricter regulatory approach. The fuel desulphurization and the use of unleaded petrol were introduced just before year 2000, while, since year 2011, it is possible to record the effects of the introduction of regional regulations on domestic heating emission control. The data were considered as representative in the previous analyzed works, since the data values were quite stable along the years, following the same

measurement conditions. A reduction of the absolute concentrations of PM is observable. Mean values were recorded of 63 μg/m^3 (PM_{10}), 38 μg/m^3 ($PM_{2.5}$) and 22 μg/m^3 (PM_1) in year 1980; 59 μg/m^3 (PM_{10}), 41 μg/m^3 ($PM_{2.5}$) and 32 μg/m^3 (PM_1) in year 2000. Finally we measured a mean value of 45 μg/m^3 (PM_{10}), 34 μg/m^3 ($PM_{2.5}$) and 29 μg/m^3 (PM_1) in year 2011. The relative errors with respect to the gravimetric data, reported from previous works, fall within a lower 1% and an upper 10% limit. On the other side, the relative distribution of PM_{10} changed. In particular, the percentages of $PM_{2.5}$ and PM_1 with respect to PM_{10} mass are: 61% ($PM_{2.5}$) and 35% (PM_1) in year 1980; 70% ($PM_{2.5}$) and 54% (PM_1) in year 2000; 75% ($PM_{2.5}$) and 65% (PM_1) in year 2011. This means that, while the aerosol emissions have changed as absolute amount, the relative emission of smaller size aerosol particles has increased over the years. It should not be disregarded that these data are referred to stable good weather conditions, when the effects of scavenging are minimal and the emissions are not removed either by transport (wind) or by wet scavenging (precipitations). Thus, the aerosol deposition is limited to gravity effect in proportion to each single particle mass. While we can observe a general relative reduction of the coarse fraction, the PM_1 have increased from 35% to 65% of the total PM_{10} mass concentrations over the 30-years period considered .

In order to provide further insights into the source identification and metal-health relationships, we carried out an ambient aerosol sampling focusing on the characteristics of trace metals in different size fractions. Three sets of size-segregated aerosol samples were collected at the centre of the city of Turin, in very different weather conditions. At the same time, VOC, NO_x and O_3 measurements were carried out in order to better assess the relationship between sources, the pollutant chemistry and the deposition processes.

The objectives of this study are: 1) to investigate the enrichment levels of selected trace metals and their size distributions, 2) to identify the major categories of sources contributing to the enrichments of trace metals, 3) to assess the influence of weather conditions on the concentrations of trace metals and their size distributions and 4) to verify their correlation with photochemical and gaseous pollutants.

Material and methods

Sampling Location and size segregated PM collection

Turin is a metropolitan area characterized by a high density of residential and commercial premises and a very high volume of vehicular traffic; several industries, including power plants, chemical plants, plastic and metallurgical factories are located on the outskirts.

Aerosol samplings were carried out in autumn and winter 2011-2012 in one site localized near the historical centre (45° 3' 6.412" N, 7° 40' 51.919" E) at an elevation of 15 meter with respect to the

road level (top roof with no other nearby buildings creating street canyon) using the 8-stages Andersen MkII nonviable cascade impactor with cut-off at: 11.0, 9.0, 5.85, 4.0, 2.7, 1.6, 0.88 and 0.54 μm of particle aerodynamic diameter. A back-up filter was mounted after the last stage. Sampling duration for each sample set was 7 days (168 hours), at a flow of 28.3 $Lmin^{-1}$ (actual conditions) as prescribed by the impactor instructions, for a total volume of sampled air of 284 m^3. The air flow was maintained with a Tecora mod. Charlie (Milan, Italy) air sampling pump. On each stage a quartz tissue filter (83 mm diameter, PALL tissuquartz 2500QAT-UP) was placed as sampling media to collect the size-segregated particulate samples. The backup filters were of the same material but with a diameter of 43 mm. Before sampling the filters were treated with ultrapure concentrated HCl at reflux for two hours, washed several times with ultrapure water and treated at 700 °C for one hour, then stored in dessicator over silica gel for 24 hours and weighed (see below). After each sampling, filters were stored in dessicator over silica gel for 24 hours before weighing, then at -18 °C until chemical analysis. Filters were weighed on a Sartorius BP 211D analytical balance with 0.01 mg resolution by using reference masses with the single pan double substitution method. PM mass was obtained as a difference between the filter after and before sampling. The procedure assures uncertainties of 0.01 – 0.03 mg (95% confidence) on PM mass. Given the volume of sampling and the uncertainty on the flow of the sampling pump (5%), the uncertainties on the PM mass concentration are in the range 0.2 – 1.2 $\mu g\ m^{-3}$.

Weather conditions (wind speed and direction, temperature, barometric pressure, relative humidity and total solar radiation) were registered at the same site.

NO_x , Volatile Organic Compounds and O_3 analysis

The analysis of NO_x, O_3 and Volatile Organic Compounds (VOC) were carried out directly on site with no intermediate sampling. O_3 and NO_x were monitored continuously by using a HORIBA ambient O_3 monitor mod APOA-360 and HORIBA NO_x monitor mod APOA-370, respectively. VOC were analyzed sampling 1.0 litre of air with an ENTECH mod. 7000 3-stage preconcentration system with water and CO_2 management (microscale purge and trap technique as suggested by the manufacturer). After preconcentration, the VOCs were detected and quantified with an Agilent Gas-chromatograph mod 6890 equipped with a 60 m, 0.32 mm I.D., 1 μm film thickness CP-SIL 5 CB column (Chrompack) and an Agilent quadrupole mass spectrometer mod 5973. The conditions were as follows: carrier gas 1.5 mL/min, column at 35 °c for 5 min, then gradient of 5.5 °C/min at 145 °C, then 40 °C/min at 245 °C (12 min). The analytical procedure is compliant with the EPA TO-15 method. Analytical standards were produced by dynamic dilution (Entech 4600A dynamic diluter, Simi Valley CA, USA) with zero grade air of a Restek (Bellefonte PA, USA) TO-15 65 Component

Mix (1 ppmv nominal of each component, including CFC-11, 12, 113 and 114). VOC analysis were performed every two hours during the 7 days PM sampling period.

Determination of Metals in size fractionated PM

The aerosol-loaded filters were digested by a microwave oven (Milestone, MLS-1200 Mega) in 100 ml tetrafluoromethoxyl vessels. The digestion mixture was composed of HNO_3 and H_2O_2 at a ratio of 4:1; nitric acid was purified by sub-boiling distillation and hydrogen peroxide was ultra-pure grade (Sigma-Aldrich). The following heating steps were applied: 1 min at 250W, 2 min at 0 W, 5 min at 200 W, 5 min at 350 W, 5 min at 550 W and 5 min at 250 W. The resulting solutions were filtered and diluted to 15 ml with Milli-Q (Millipore) ultrapure water (18.2 MΩ cm).

As, Cd, Co, Cr, Cu, Fe, Mn, Mo, Ni, Pb, Pd, Pt, Rh, Sn, V and Zn were determined by a magnetic sector inductively coupled plasma mass spectrometer (SF-ICPMS, Thermo Finnigan Element 2). Mass resolution and isotope selection were optimized for each element to ensure resolution of spectral interferences and maximize sensitivity. A minimum of triplicate 180 s analyses on each sample was conducted following a 60 s uptake and stabilization period. Between samples the nebulizer system was rinsed for 2 min with 2% sub-boiling HNO_3, which eliminated carry-over and reconditioned the sampler cone. Sets of instrumental blank and calibration verification checks were run at frequent intervals during the batch sequence. The calibrations were performed with standard solutions prepared in aliquots of sample blanks. Process blanks were incorporated into the dissolution and analytical procedure to assess metal contribution from the filters, bombs, Milli-Q water and purified acids used in this procedure. All signals for samples were obtained after subtraction of their appropriate process blank values. The relative standard deviation for all elements in each sample was always lower than 5 %.

NIST SRM 1648a (Urban Particulate Matter) was used to verify that analyte concentrations were within 15% of the expected values before proceeding with sample analysis.

Results and discussion

Weather conditions

In this study three sampling periods, namely in October, January and February, were carried out in different weather conditions. Mean meteorological variables are reported in Table 1, Table 2 and Table 3. Hourly data are reported in the supplementary material (Figure S-1, Figure S-2, Figure S-3).

The first (October) sampling has been performed when typical late summer weather was present, with clear skies, high temperature, but with strong temperature gradient between day and night and high night relative humidity with the formation of mists. Concerning wind speed and direction, it is noteworthy that it was under 2.5 m/s for the first four days of sampling whereas it increased on the fifth day, when a strong katabatic wind from WNW carried air masses of alpine origin, decreasing both the temperature (5 °C decrease) and the relative humidity (RH) (from 70 to 44%).

The second (January) sampling occurred in early winter climatic conditions. The weather conditions were stable, with temperatures below 0 °C only during the night. During this sampling (in the fourth day) a Foehn episode occurred, increasing temperature, atmospheric mixing and lowering relative humidity. The mean RH dropped from about 80% to 55% with minima under 35%.

Both katabatic wind and Foehn caused the transport of aged air masses from WNW.

The third (February) sampling took place during the early 2012 european cold wave (World Meteorological Organization, 2012). This period started on 28 January and ended on 17 February and was characterized by extremely cold condition. In the nearby of Turin temperature as low as -20 °C were registered, with temperatures continuously under 0 °C. This was one of the most cold periods of the last century (being the other in February 1956 and February 1985). During the first days of cold spell a heavy snow episode occurred (January 28 - February 2), scavenging efficiently airborne particulate matter. Therefore, the weather conditions were significantly different with respect to the previous sampling periods. The temperature remained always below zero with stable weather conditions and sunny with very little wind. Low temperatures delayed the snow melting until the end of sampling, greatly increasing the albedo. As a result, the high actinic flux from the snow cover increased the atmospheric photochemical reactivity at ground level, as well as it is known that snowpack can favour photochemical reactions of pollutants adsorbed onto the hydrometeors (e.g. nitrate) (Grannas et al., 2007; Neemann et al., 2014).

O_3, NO_x

The time profiles of NO_x and O_3 are quite different for the three sampling periods, due to relevant differences in the atmospheric conditions and solar radiation, that alter not only the dilution and transport of pollutants, but also the deposition processes and efficiencies. The time profiles with hourly resolution are reported in the supplementary material (Figure S-4, Figure S-5, Figure S-6). The mean concentrations over the entire sampling periods are reported in Table 4. Po valley is the European region with the highest level of photochemical pollution in summer due to the presence of high density of anthropogenic activities and associated emissions (mainly NO_x), along with the presence of relevant emissions of highly reactive biogenic VOCs from the surrounding alpine

regions. Furthermore the particular geographic conformation prevents an efficient dispersion of primary pollutants. In summer 2011 more than 30 exceedances of the 120 μg m^{-3} (56 ppbv) O_3 EU limit (as 8 hours running average) occurred in >90% of the measuring stations of Po valley (EEA 2013). The October data are typical of medium photochemical processing of in situ emitted pollutants (stable air masses), with mean concentration of NO (10 ppbv) under the mean concentration of NO_2 and O_3 (22.9 and 19.3 ppbv, respectively). NO_2 average level exceeded the EU annual average limit (19.5 ppbv or 40 μg m^{-3}). Two daily peaks of primary pollutants were observed (see also the next section) during rush hours (early morning and late afternoon). Secondary pollutants (NO_2 and O_3) show two daily peaks as well, but broader and with a lag with respect to the peaks of NO. During the katabatic wind episode, the intrusion of aged air masses from WNW and the dilution of the primary pollutants emitted in the urban context cut down the concentration of NO, keeping it constant and relatively high during all the fifth day.

The January data are typical of winter days, with no precipitations, stable air masses with low mixing height, strong temperature inversion and low solar radiation. In these conditions the primary pollutants prevail, indeed the O_3 concentrations are very low with quite high NO concentrations. O_3 levels increased from under 2 ppbv to 25 ppbv on the third-fourth days due to the Fohen episode, that transported aged air masses from WNW thereby increasing mixing, strongly lowering NO concentration.

The February data are somewhat unusual due to the presence of a stable snow cover in the urban environment and temperature constantly under 0 °C. During this period the city was permanently snow covered, except for the road surfaces. As a result, at least 70% of the urban area and more than 90% of the surrounding rural areas were covered by snow. Mean concentrations of NO, NO_2 and O_3 point out to a discrete photochemical processing of primary pollutants, being NO and NO_2 levels very similar. The time profiles of these pollutants show daily cycles very similar to those observed in October, confirming the photochemical conversion, being the O_3 level limited by the higher level of NO_x and by low levels of humidity, but with a manifest daily maximum in late afternoon. The presence of the snow cover affects the surface albedo, atmospheric circulation and dry deposition efficiencies of pollutants. Similar episodes of high winter ozone in the presence of snow cover were registered in close basins (see for example Neeman et al 2014), due to enhanced boundary layer stability and available solar radiation. Indeed the max solar radiation data are very similar to those of October 2011 (Table 1 and Table 3), but in February the albedo of the snow cover makes available also a relevant intensity of reflected radiation. Moreover, the dry deposition velocities of many pollutants are one order of magnitudes lower for snow covers and frozen soils with respect to soil and sand (Galbally I.E. et al. 1980, De Leeuw et al., 1990). Snow photochemistry of pollutant

entrapped in the snow flakes during precipitation makes the snow cover a relevant source of secondary pollutants, including NO_x (Grannas et al., 2007; Neemann et al., 2014). Enhanced production of secondary aerosol is thus expected.

Volatile Organic Compounds

During the three sampling periods the concentration of hexane, isooctane, as well as benzene, toluene, xylenes and ethylbenzenes (BTEX) were determined. These compounds are mainly emitted in the exhaust of gasoline powered motor vehicles (Monod et al, 2001; Schauer et al, 2002). Moreover BTEX are precursors of secondary organic aerosol (Kroll et al. 2008, Bahreini et al, 2012, Donahue et al. 2009, Ng N.L et al 2007) and the ozone production in urban environment is often under a VOC limited regime. The time profiles of VOC mixing ratios with two hours resolution are reported in the supplementary material (Figure S-7, Figure S-8, Figure S-9). The average concentrations over the entire sampling periods are reported in Table 5. For comparison the mixing ratios of CFC-11, CFC-12 and CFC-113 are also reported. The time profiles of these compounds are flat (data not reported) and the measured concentrations are slightly higher than the average concentrations reported in the northern hemisphere (Bullister, 2014), assuring the quality of the data.

The highest concentrations of VOCs were recorded during the January campaign, and they could be ever higher if the Fohen episode during days 4-5 had not took place, whereas, somewhat surprisingly, the lowest concentrations were observed during the February campaign. The October time profiles (Figure S-7) shows two daily peaks in rush hours, highly correlated with NO time profiles and in advance with respect to ozone peaks, indicating local photochemical processing. As stated in the preceding paragraph, the WNW katabatic wind during days 4-5 caused the intrusion of aged air masses and the drop in primary pollutants mixing ratios. During the January campaign the lower solar radiation and stable atmospheric conditions (except in days 4-5 due to the Fohen), favoured accumulation of primary pollutants. VOCs profiles during the first three days show a broad peak during daytime.

The snow cover during February, slowing down the deposition rates of O_3 and increasing the availability of solar radiation at ground, enhanced photochemical reactivity at ground/top roofs level. The time profiles of O_3, NO_x and VOCs were very similar to typical photochemical smog episodes. Thus a relevant production of secondary organic aerosol is expected.

Mass distribution of the PM

Figure 1 shows the gravimetric size distribution of airborne particulate matter collected in February sampling. The other mass distributions for October and January samplings were not determined.

PM_{10} distribution is bimodal, with modes around 5 μm and 1 μm, indicating an input from several sources (vehicular traffic and/or fossil fuel combustion processes, as well as secondary formation) and typical of urban aerosols (Allen et al., 2001; Keywood et al., 1999; Taiwo et al., 2014). It is also present a just outlined mode for PM greater than 10 μm. However, the accumulation mode (around 1 μm) is by far the highest. Indeed, by integrating data we note that $PM_{2.5}$ represents already 80% of the total mass of PM collected; this percentage increases to 92% with PM_{10} while it is only 8% for the largest PM. These results are comparable with PM_{10} concentrations determined by the monitoring stations of the Italian Regional Agency for Environmental Protection (ARPA) for the same sampling period.

This pattern is likely due to the meteorological conditions present during sampling period (temperature constantly under 0°C, low wind speed, presence of a snow cover) reducing vertical circulation, thereby lowering the mixing layer thickness, reducing deposition rates and enhancing production of secondary aerosols, thus promoting accumulation of fine suspended particles at ground level. Moreover, gas to particle conversion of emissions from motor vehicles and from household heating systems is stimulated at low temperature (Mulawa et al., 1997).

Size distribution of elements associated to time integrated PM samples

The average elemental concentrations, expressed in ng/m^3, measured in the three sampling periods (October 2011, January 2011 and February 2011) in Turin are reported in Table 6, together with those detected in other Italian and European towns (Vecchi et al., 2007; Dongarrà et al., 2007; Bocca et al., 2003; Toscano et al., 2011; Johansson et al., 2009; Heal et al., 2005; Querol et al., 2001). Most of the elements present lower concentrations in Turin than in other considered urban areas; this is in part due to the decreasing trend associated to the recent European directives for the control of emissions into the atmosphere have been applied for longer times. Taking into account the great variability present in atmospheric conditions, it is however possible to state that the element concentrations in Turin atmospheric particulate matter are similar to those of the other considered towns.

The highest metal concentrations in atmospheric PM samples were reached by Cr (0.83 ng/m^3), Zn (32.7 ng/m^3), Cd (1.85 ng/m^3), Sn (30.2 ng/m^3) and Pt (0.03 ng/m^3) in October sample; Co (0.06 ng/m^3), Ni (1.55 ng/m^3), Cu (2.52 ng/m^3), As (0.13 ng/m^3), Mo (0.34 ng/m^3) and Pb (2.25 ng/m^3) in January sample; and V (0.30 ng/m^3), Mn (3.10 ng/m^3), Fe (207 ng/m^3), Rh (0.02 ng/m^3) and Pd (0.03 ng/m^3) in February sample.

The elements having a higher variability among the three sampling periods were vanadium, cobalt, arsenic, rhodium, cadmium and tin, i.e. those that are most likely emitted by combustion processes, with the exception of rhodium. The high variability of this last element, instead, could be an artifact due to its low concentration, close to the instrumental detection limit (0.5 pg/m^3).

Figure 2 shows the size distributions of elements for the three sampling periods carried out.

First of all, it can be noted that there is a greater difference in element size distribution between the first sampling (October) and the last two (January and February), despite the last sampling having been performed in the days immediately following a heavy snowfall. Evidently the difference existing among the sources influencing the element size distribution of Turin airborne particulate matter in autumn and winter seasons is more significant than the scavenging effect of a snowfall on PM. Indeed, elements, such as Co, V and partially Ni, typical markers of fossil fuels combustion processes, show a larger mode in the finest fraction (< 1.6 μm) in winter than in autumn. This behaviour can be ascribed both to higher emissions from the combustion of fossil fuels in heating systems and to persistent thermal inversions at ground level occurring in Northern Italy during the winter, as reported in various studies (Marcazzan et al., 2001; Toscano et al., 2011; Malandrino et al., 2013). Conversely, zinc and rhodium present larger mode in the fine fraction (< 2.7 μm) in autumn; this can probably be attributed to an increased concentration of fine particles emitted into atmosphere from vehicular traffic. Many studies stated that zinc in the air is generated by road dust resuspended by vehicular movement, vehicle exhaust emissions and tyre wear (Pakkanen et al., 2001; Birmili et al., 2006). Rh, instead, together with Pd and Pt, the so-called Platinum-Group Elements (PGEs), is contained in the catalytic converters for automotive traction. Three way catalytic (TWC) converters for Otto cycle engines contain only Pd and Rh in ratios from 2:1 to 5:1. Diesel Oxidation Catalysts (DOC) and Nitrogen Storage Catalysts (NSC) for diesel engines contain principally Pt and Pd (10 to 1-2 and 2:1, respectively) with only traces of Rh. These elements are emitted primarily as particulate matter in consequence of the thermal and mechanical losses of the catalytic material when the engine is working. For this reason, traffic can be considered the main source of PGEs contamination of urban areas (Bocca et al., 2003; Artelt et al., 2000). To confirm this explanation it is worth to note that, if we consider only the Pt size distribution in the fine fraction, also this element presents a higher concentration in the < 2.7 μm fraction in the autumn period.

A possible explanation for Zn and Rh seasonal size distribution is the greater influence of road dust and vehicular traffic on the fine fraction in autumn owing to the lower humidity in the air in this season than in winter; this can induce a greater suspension and persistence of the particles emitted by vehicles into the air. This assumption is supported by relative humidity (RH%) values recorded

in the sampling periods: they are lower in October (average RH% = 63) than in January and February (average RH% = 73 and 76 respectively).

The PM_{10} concentrations of Pt (20 pg m^{-3}) and Pd (26 pg m^{-3}) in the Turin urban atmosphere are within the ranges (1.3–23 pg m^{-3} for Pt and 0.8–51.4 pg m^{-3} for Pd) reported in urban atmosphere sampled globally since 1998 to 2003 (Rauch et al., 2005). Although Pd and Pt are often below detection limits, these results are in agreement with the data collected by Rauch et al. (2005) showing typical Pt/Pd ranges of 0.2 – 2.9 in urban air particles. Instead, the PM_{10} concentration of Rh (9 pg m^{-3}) exceeds these limits (the highest value reported in Rauch et al. (2005) is 4.2 pg m^{-3}). A possible explanation to this behaviour can be due to a higher contribution of this element in atmosphere from crustal sources particularly in winter period; indeed, this element is characterized by a high mode in coarse fraction in both winter samplings.

Overall, on the basis of the size distributions, elements could be divided into three groups. Group 1 elements are mostly concentrated in coarse mode (2.7 – 11 μm), including Cd, Cr, Cu, Fe, Mn, Mo, Pt and Sn; Group 2 elements show higher concentrations in accumulation mode (< 2.7 μm), including As, Co, Pb and V; Group 3 elements present several modes spread throughout the size distribution including Ni, Pd, Rh and Zn. This behaviour is generally in line with the findings reported by other authors (Wang et al., 2006; Duan et al., 2012, Samara et al., 2006); however, the size distribution of some elements was different in the three sampling periods, as reported above.

Enrichment Factors (EFs) of elements in aerosol relative to Earth's crustal composition were calculated according to:

$$EF = (C_{Me} / C_{Fe})_{sample} / (C_{Me} / C_{Fe})_{Crust}$$

where $(C_{Me}/C_{Fe})_{sample}$ is the concentration ratio of the metal and Fe in the investigated sample and $(C_{Me}/C_{Fe})_{Crust}$ is the same ratio in Earth upper-crust as reported by Wedepohl (1995). We used crustal Fe level as a reference since soil is considered to be the major source of Fe in aerosol. These values were employed to assess the extent of non-crustal contributions to the elemental concentration levels for the three groups. However, it must be mentioned that EFs only provide qualitative information on element sources because of the wide variation in concentrations in the upper crust (Contini et al., 2010).

As shown in Figure 3, Group 1 elements present different enrichment factors indicating the lack of a common source for all. Indeed, Cr, Fe and Mn show low EFs in both coarse and fine mode. Therefore they are mainly originated from crustal sources. Their percentages in the coarse fraction ranged from 69 % (Mn) to 79 % (Cr) as average values, but they were higher in October and

January (from 77 % for Mn to 92 % for Fe) than in February (from 49 % for Mn to 73 % for Cr), likely to indicate a greater effect of the snowfalls on PM having coarser mode (> 2.7 μm) and crustal origin.

Instead, the EFs of the other Group 1 elements (Cd, Cu, Mo, Pt and Sn) are high both in coarse and (mainly) in accumulation mode, suggesting that their sources are mainly anthropogenic activities and, at lesser degree, soil dust. In particular, these elements might mainly come from the re-suspended soil containing previously deposited PM and vehicle exhaust emissions.

Group 2 elements show a higher concentration in fine fraction particularly in winter and, therefore, they should be related to fossil fuel combustion processes, likely in household and industrial heating systems. It is interesting to note that their EFs are not high both in coarse and in accumulation mode, but they increase by approximately an order of magnitude between the two fractions (e.g. for vanadium, the EFs for coarse and fine fractions are 0.3 and 3.6 respectively) to indicate a possible anthropogenic contribution in fine fraction. In more detail, As and Pb are characterized by homogeneous size distribution and similar EFs over time, whereas the size distribution and the EFs for V and Co change over time, more precisely their EFs are higher in January sampling and their concentrations in the accumulation fraction are clearly greater in winter than in autumn. This scenario allows us to assume that these elements derive from different combustion sources. Many researchers have indicated multiple sources for Pb in airborne particulate matter: vehicle emission, steel manufacturing, waste disposal and incineration, non-ferrous metal production, coal and oil combustion (Mishra et al., 2004; Al-Masri et al., 2006; Lim et al., 2010). Regarding As, Yli-Tuomi et al. (2003) reported the use of this element as a marker for non-ferrous metal refinery smelting processes. Moreover Chueinta et al. (2000) assigned As as marker for coal combustion and V for oil combustion. Ni, V and Co are widely used as markers for the combustion of heating fuel (Vallius et al., 2005).

Taking this into account it is possible to assume that these elements are emitted in fossil fuel combustion processes by coal and heavy oil inside the industrial complexes (Pb and As) and by heating oil in household heating systems (V and Co).

Ni, Pd, Rh and Zn, instead, present a bimodal distribution indicating an input from several sources (local traffic and/or fossil fuel combustion processes). The EFs for Pd, Rh and Zn are very high both in coarse and in accumulation mode: this indicates a predominance of anthropogenic sources for these elements in both fractions. Taking into account that traffic is the main source of pollution by PGEs in populated areas and that the presence of zinc in the air is often associated to vehicular traffic, resuspended road dust, vehicle exhaust emission and tyre wear, it is possible to suppose a common origin for these elements influencing both coarse and accumulation fraction: vehicular

traffic and resuspended road dust, containing previously deposited PM. With regard to nickel, even if the size distribution of this element is bimodal, it presents a high EF only in accumulation mode. Therefore, it is possible to suppose that it is emitted by multiple sources: fossil fuel combustion in motor vehicles and in household heating systems to a greater degree and road dust to a lesser degree.

Overall, As, Co, Ni, Pb, V and Zn were found in large proportions in particle size below 0.88 μm and could therefore deposit mainly into the alveoli region of human respiratory system. The presence of some among the more toxic elements in the finer PM sizes in all the samples indicates that Turin urban atmospheric PM is capable of causing both proximal and distal contamination, and individual particles are small enough to be easily inhaled into deep lung zones (Romanazzi et al, 2014).

Chemometric data analysis

In an effort to better identify the possible sources that influence the chemical composition of PM_{10} and to evidence the impact of weather conditions on the concentrations of trace metals and their size distributions, a chemometric treatment of the experimental data was carried out through the application of a well-known statistical multivariate analysis technique: principal component analysis (PCA). It is an established method for aerosol analysis after its first application to aerosol source apportionment (Thurston and Spengler, 1985). Its strength is that it is based on the evolution of data collected in a specific site, and an a priori knowledge about sources is not required. This data elaboration has been performed with XlStat 2013.2.04 software package.

The chemometric study was carried out considering the total data set (27 samples with 15 variables). Only the chemical species with concentrations above the detection limit in more than 70% of the samples were included in the dataset; therefore Rh was excluded from the multivariate analysis. A value generated applying NIPALS (Nonlinear Iterative Partial Least Squares) method was inserted for concentrations below the detection limit in order to thoroughly apply PCA and HCA without losing any data and, at last, the data set was auto-scaled.

Figure 4 a and b show respectively the score and loading plot obtained by PCA. Taking into account the scree plot, we have reported only the first two principal components that contain a total variance of about 50%; all the others PCs contain a low, and therefore not significant, percentage of information. The numbers from 0 to 8 reported beside sampling date in each sample indicate its size range, respectively from 11 to < 0.54 μm.

As all the samples having size range less to 2.7 μm have negative values on PC1, it is possible to hypothesize that this component is related to the size distribution of Turin airborne particulate

matter. Instead, as almost all samples collected in February take positive values on PC2, with the exception of the first two samples (Feb 0 and Feb 1), relating to the atmospheric particles having greater diameter, and all the samples collected in October take negative values on PC2, with the exception of the first one (Oct 0), we can hypothesize that the second component is related to sampling period. Overall we observe a differentiation between the samples collected in winter (January and February) and in autumn period (October) and, within each of the two clusters, between the samples having size range less to 2.7 μm and the other ones. This distribution permits to affirm that the element composition of airborne particulate matter of Turin depends on the sampling period: the samples collected in winter are influenced by most of the variables (elements) considered, suggesting a higher input of pollutants due to thermal inversion, to a larger use of household heating systems and to the fact that the conversion of emissions from motor vehicles into particulate matter is stimulated at low temperature (Mulawa et al., 1997). Moreover a clear separation between coarse and fine particles is evident in all the samplings, but it is to be noted that the particle size distribution in the two winter samplings is very similar and differs from that characterizing the autumnal sampling. Furthermore the fine particles collected in winter are characterized by high concentrations of Group 2 elements (As, Co, Ni, Pb and V), which are considered markers of the fossil fuel combustion source, whereas the coarse particles are much more influenced by iron and manganese, typical crustal elements, and by Cu, Mo, Pd and Pt, elements usually connected with vehicular emissions and road dust. Instead, the fine particles collected in autumn are characterized by low loadings for most of the elements considered with the exception of the Oct 8 sample, influenced by the variable identified by the vector of arsenic. This behaviour is a further confirmation of the influence of sampling period discussed previously and of the different source of As, likely linked to fossil fuel combustion processes inside industrial complexes. Finally, the coarse particles of autumn sampling are more scattered than those collected in winter. In particular the Oct 0 sample is strongly influenced by crustal elements (i.e. Fe and Mn) indicating likely a greater input of soil dust transported by wind also from long distance. The other samples are aligned with the direction of Pd, Cd and Sn vectors, having a unquestionable anthropogenic origin, possibly due to vehicular traffic.

Regarding variables, it is interesting to note that all the variables related to fossil fuel combustion processes, i.e. Ni, V, Co, Pb and As, are represented by vectors having direction opposite, relative to PC1, to those of most of the other elements to confirm their clearly different sources. Moreover it is possible to observe that the correlations between V and Co and between Pb and As are the highest (Pearson correlation coefficients for $\alpha = 0.05$ are 0.83 and 0.68 respectively) among those calculated for the above reported elements: this confirms different combustion sources for these

elements, i.e. household heating systems for V and Ni and industrial combustion processes for Pb and As. Finally the correlation between Co and Ni (Pearson correlation coefficient for $\alpha = 0.05$ is 0.60) is possibly due to a combustion source, but the content in Ni is also related to traffic. A correlation between Mn and Fe is evident, suggesting a common origin due to the input of soil dust transported by wind. The correlation among Pt, Pd, Mo and Cu could indicate a common source linked to the emissions by vehicular traffic and road dust. Chromium is partially correlated with both the crustal and anthropogenic elements, suggesting an input from several sources (local traffic and soil dust). The correlation between Cd and Sn is very likely reflecting their anthropogenic origin, possibly due to industrial emissions and/or vehicular traffic. Finally the direction of the vector representing the variable zinc is more difficult to interpret because it is not correlated with other elements: this is likely due to the fact that a well-defined trend is not observable for this element, since it can be emitted by multiple sources (e.g. industrial, road dust and traffic).

Conclusions

The concentrations of 16 elements (As, Cd, Co, Cr, Cu, Fe, Mn, Mo, Ni, Pb, Pd, Pt, Rh, Sn, V and Zn) in eight size fractions of urban airborne particulate matter collected in Turin (Italy) were determined during two sampling periods reflecting late summer and winter weather conditions. A third winter measurement period took place after the early 2012 european cold wave, with very unusual conditions (persistent snow cover, temperatures constantly under 0 °C, clear sky and stable atmosphere). The size distribution of elements in all the sampling periods allowed the identification of three main behavioural types: (a) elements found mainly within coarse particles (Cd, Cr, Cu, Fe, Mn, Mo, Pt and Sn); (b) elements found mainly within fine particles (As, Co, Pb and V) and (c) elements with several modes spread throughout the entire size range (Ni, Pd, Rh and Zn).

The clustering of the scores obtained by Principal Component Analysis indicates that the element distribution as a function of the PM aerodynamic diameter in Turin strongly depends on the sampling period. Moreover the chemometric analysis confirms that, for elements investigated, it is more evident a separation between the two winter samplings and the autumnal sampling, proving that the metal particle size distribution is less influenced by particular weather phenomena like the strong snowfall happened during February sampling than other atmospheric pollutants. Finally the correlations observed between the inorganic elements permit to infer about their origin.

The concentration levels gaseous trace pollutants, namely O_3, NO_x and VOCs, are scarcely correlated with the metal contents of all the size classes of the PM. The differences found in the O_3, NO_2 and VOCs levels of the two winter campaigns due to the relevant photochemical reactivity in the period after the snow episode, do not reflect in differences in the metals distribution in the PM.

Since PM metals, NO_x and VOC have common sources, this behaviour can be ascribed to relevant differences in the transformation and deposition processes.

Acknowledgment

VM, MM, CM and AO acknowledge financial support from Università di Torino - Ricerca Locale.

Supplementary Data

Additional information as noted in text. Supplementary Information associated with this article can be found, in the online version, at http://xxxxxxxxxxxx

References

Allen A.G., Nemitz E., Shi J.P., Harrison R.M., Greenwood J.C., 2001. Size distribution of trace metals in atmospheric aerosols in the United Kingdom. Atmos. Environ. 35, 4581-4591.

Al-Masri M.S., Al-Kharfan K., Al-Shamali K., 2006. Speciation of Pb, Cu, and Zn determined by sequential extraction for identification of air pollution sources in Syria. Atmos. Environ. 40, 753–761.

Artelt S., Levsen K., König P., Rosner G., 2000. in Anthropogenic Platinum-Group Element Emissions and Their Impact on Man and Environment, ed. F. Alt and F. Zereini, Springer-Verlag, Berlin, 33.

Bahreini R., Middlebrook A. M., de Gouw J. A., Warneke C., Trainer M., Brock C. A., Stark H., Brown S. S., Dube W. P., Gilman J. B., Hall K., Holloway J. S., Kuster W. C., Perring A. E., Prevot A. S. H., Schwarz J. P., Spackman J. R., Szidat S., Wagner N. L., Weber R. J., Zotter P., Parrish D. D., 2012. Gasoline emissions dominate over diesel in formation of secondary organic aerosol mass. Geophys. Res. Lett. 39, L06805.

Baulig A., Singh S., Marchand A., Schins R., Baroukic R., Garlatti M., Marano F., Baeza-Squiban A., 2009. Role of Paris PM2.5 components in the pro-inflammatory response induced in airway epithelial cells. Toxicology 261, 126-135.

Birmili W., Allen A.G., Bary F., Harrison R.M., 2006. Trace metal concentrations and water solubility in size-fractionated atmospheric particles and influence of road traffic. Environ. Sci. Technol. 40, 1144-1153.

Bocca B., Petrucci F., Alimonti A., Caroli S., 2003. Traffic-related platinum and rhodium concentrations in the atmosphere of Rome. J. Environ. Monit. 5, 563–568.

Bullister J. 2014, Atmospheric CFC-11, CFC-12, CFC-113, CCl4 and SF6 Histories (1910-2014). http://cdiac.ornl.gov/oceans/new_atmCFC.html. Last accessed 18 february 2015

Casazza M., Gilli G., Piano A., Alessio S., 2013. Thirty-years assessment of size-fractionated particle mass concentrations in a polluted urban area and its implications for regulatory framework. J. Environ. Accounting and Management 1, 259-267.

Chueinta W., Hopke P.K., Paatero P., 2000. Investigation of sources of atmospheric aerosol at urban and suburban residential areas in Thailand by positive matrix factorization. Atmos. Environ. 34, 3319–3329.

Contini D., Genga A., Cesari D., SicilianoM., Donateo A., Bove M.C., Gualcito, M.R., 2010. Characterization and source apportionment of PM10 in an urban background site in Lecce. Atmos. Res. 95, 40–54.

De Leeuw F.A.A.M., Van Rheineck Leyssius H.J., 1990 Modeling Study of SO_x and NO_x Transport during the January 1985 smog episode, Wat. Air Soil Pollution 51, 357-371.

Donaldson K., Brown D., Clouter A., Duffin R., MacNee W., Renwick L., Tran L., Stone V, 2002. The pulmonary toxicology of ultrafine particles. J. Aerosol Med. 15, 213-220.

Donahue N.M., Robinson A.L., Pandis S.N., 2009. Atmospheric organic particulate matter: From smoke to secondary organic aerosol. Atmos Environ 43, 94-106

Dongarrà G., Manno E., Varrica D., Vultaggio M. 2007. Mass levels, crustal component and trace elements in PM10 in Palermo, Italy, Atmos. Environ. 41, 7977–7986.

Duan J., Tan J., Wang S., Hao J., Chai F., 2012. Size distributions and sources of elements in particulate matter at curbside, urban and rural sites in Beijing. J. Environ. Sci. 24, 87-94.

Englert N., 2004. Fine particles and human health – a review of epidemiological studies. Toxicol. Lett. 149, 235-242.

EEA (European Environment Agency), 2013. Air quality in Europe – 2013 report 9/2013. Copenhagen: European Environment Agency, ISBN 978-92-9213-406-8, ISSN 1725-9177, doi:10.2800/92843. http://www.eea.europa.eu/publications/air-quality-in-europe-2013, last accessed 16 february 2015.

Galbally I.E., Roy C.R., 1980. Destruction of ozone at the earth's surface. Quarterly J. Royal Meteorol. Soc. 106, 599-620

Grannas A.M., Jones A.E., Dibb J., Ammann M., Anastasio C., Beine H.J., Bergin M., Bottenheim J., Boxe C.S., Carver G., Chen G., Crawford J.H., Dominé F., Frey M.M., Guzmán M.I., Heard D.E., Helmig D., Hoffmann M.R., Honrath R.E., Huey L.G., Hutterli M., Jacobi H.W., Klán P., Lefer B., McConnell J., Plane J., Sander R., Savarino J., Shepson P.B., Simpson W.R., Sodeau J.R., von Glasow R., Weller R., Wolff E.W., Zhu T., 2007. An overview of snow photochemistry: evidence, mechanisms and impacts, Atmos. Chem. Phys., 7, 4329–4373.

Handler M., Puls C., Zbiral J., Marr I., Puxbaum H., Limbeck A., 2008. Size and composition of particulate emissions from motor vehicles in the Kaisermuhlen-Tunnel, Vienna. Atmos. Environ. 42, 2173-2186.

Heal M.R., Hibbs L.R., Agius R.M., Berland I.J., 2005. Total and water-soluble metal content of urban background PM10, PM2.5 and black smoke in Edinburgh, UK. Atmos. Environ. 39, 1417–1430.

Johansson C., Norman M., Burman L., 2009. Road traffic emission factors for heavy metals. Atmos. Environ. 43, 4681–4688.

Katsouyanni K., Touloumi G., Samoli E., 2001. Confounding and effect modification in the short-term effects of ambient particles on total mortality: results from 29 European cities within the ALPHEA2 Project. Epidemiology 12, 521-531.

Keywood M.D., Ayers G.P., Gras J.L, Gillett R.W., Cohen D.D., 1999. Relationships between size segregated mass concentration data and ultrafine particle number concentrations in urban areas. Atmos. Environ. 33, 2907-2913

Krewski D., Rainham D., 2007. Ambient Air Pollution and Population Health: Overview. J. Toxicol. Env. Heal. A, 70, 275–283.

Kroll J.H., Seinfeld J.H., 2008. Chemistry of secondary organic aerosol: Formation and evolution of low-volatility organics in the atmosphere. Atmos. Environ. 42, 3593–3624

Lall R., Kendall M., Ito K., Thurston G.D., 2005. Estimation of historical PM2.5 exposures for health effects assessment. Atmos. Environ., 38, 5217-5226.

Lim J.M., Lee J.H., Moon J.H., Chung Y.S., Kim K.H., 2010. Source apportionment of PM10 at a small industrial area using Positive Matrix Factorization. Atmos. Res. 95, 88–100.

Malandrino M., Di Martino M., Ghiotti G., Geobaldo F., Grosa M.M., Giacomino A., Abollino O., 2013. Inter-annual and seasonal variability in PM10 samples monitored in the city of Turin (Italy) from 2002 to 2005. Microchem. J. 107, 76–85.

Marcazzan G.M., Vaccaro S., Valli G., Vecchi R., 2001. Characterization of PM10 and PM2.5 particulate matter in the ambient air of Milan (Italy). Atmos. Environ. 35, 4639–4650.

Masiol M., Squizzato S., Ceccato D., Pavoni B., 2015. The size distribution of chemical elements of atmospheric aerosol at semi-rural coastal site in Venice (Italy). The role of atmospheric circulation. Chemosphere,119, 400-406.

Maté T., Guaita R., Pichiule M., Linares C., Diaz J., 2010. Short-term effect of fine particulate matter (PM2.5) on daily mortality due to diseases of the circulatory system in Madrid (Spain). Sci. Tot. Env., 408, 5750-5757.

Mishra V.K., Kim K.H., Kang C.H., Choi K.C., 2004. Winter time sources and distribution of airborne lead in Korea. Atmos. Environ. 38, 2653–2664.

Monod A., Sive B.C., Avino P., Chen T., Blake D.R., Rowland F.S., 2001. Monoaromatic compounds in ambient air of various cities: a focus on correlations between the xylenes and ethylbenzene. Atmos. Environ. 35, 135-149.

Mulawa P.A., Cadle S.H., Knapp K., Zweidinger R., Snow R., Lucas R., Goldbach J., 1997. Effect of ambient temperature and E-10 fuel on primary exhaust particulate matter emissions from light-duty vehicles. Environ. Sci. Technol. 31, 1302–1307.

Neemann E.M., Crosman E.T., Horel J.D., Avey L., 2014. Simulations of a cold-air pool associated with elevated wintertime ozone in the Uintah Basin, Utah. Atmos. Chem. Phys. Discuss., 14, 15953–16000.

Ng, N.L., Kroll, J.H., Chan, A.W.H., Chhabra, P.S., Flagan, R.C., Seinfeld, J.H., 2007. Secondary organic aerosol formation from m-xylene, toluene, and benzene. Atmospheric Chemistry and Physics 7, 3909–3922.

Pakkanen T., Loukkola K., Kohonen C., Aurela M., Mäkelä T., Hillamo R., Aarnio P., Koskentalo T., Kousa A., Maenhaut W., 2001. Sources and chemical composition of atmospheric fine and coarse particles in the Helsinki area. Atmos. Environ. 35, 5381–5391.

Querol X., Alastuey A., Rodriguez S., Plana F., Ruiz C.R., Cots N., Massagué , G., Puig, O., 2001. PM10 and PM2.5 source apportionment in the Barcelona Metropolitan area, Catalonia, Spain. Atmos. Environ. 35, 6407–6419.

Rauch S., Hemond H., Peucker-Ehrenbrink B., Ek K.H., Morrison G., 2005. Platinum group element concentrations and osmium isotopic composition in urban airborne particles from Boston, Massachusetts. Environ. Sci. Technol. 39, 9464-9470.

Ramgolan K., Chevaillier S., Marano F., Baeza-Squiban A., Martinon L., 2008. Proinflammatory effect of fine and ultrafine particulate matter using size-resolved urban aerosols from Paris. Chemosphere 72, 1340-1346.

Romanazzi V., Casazza M., Malandrino M., Maurino V., Piano A., Schilirò T., Gilli G., 2014. PM10 size distribution of metals and environmental-sanitary risk analysis in the city of Torino. Chemosphere 112, 210–216.

Samara C., Voutsa D., 2006. Size distribution of airborne particulated matter and associated heavy metals in the roadside environment. Chemosphere 59, 1197-1206.

Sánchez de la Campa A.M., Moreno T., de la Rosa J., Alastuey A., Querol X., 2011. Size distribution and chemical composition of metalliferous stack emissions in the San Roque petroleum refinery complex, southern Spain. J. Hazard. Mater. 190, 713-722.

Schauer J.J., Kleeman M.J., Cass G..R., Simoneit B.R., 2002. Measurement of Emissions from Air Pollution Sources. 5. C1-C32 Organic Compounds from Gasoline-Powered Motor Vehicles. Environ. Sci. Technol. 36, 1169-1180

Song F., Gao Y., 2011. Size distributions of trace elements associated with ambient particular matter in the affinity of a major highway in the New Jersey-New York metropolitan area. Atmos. Environ. 45, 6714-6723.

Taiwo A.M., Beddows D.C.S., Shi Z., Harrison R.M., 2014. Mass and size distribution of particulate matter components: comparison of an industrial site and an urban background site. Sci. Tot. Env. 475, 29-38.

Thurston G.D., Spengler J.D., 1985. A quantitative assessment of source contributions to inhalable particulate matter pollution in metropolitan Boston. Atmos. Environ. 19, 9–25.

Toscano G., Moret I., Gambaro A., Barbante C., Capodaglio G., 2011. Distribution and seasonal variability of trace elements in atmospheric particulate in the Venice Lagoon. Chemosphere, 85, 1518-1524.

Vallius M., Janssen N.A.H., Heirich J., Hoek G., Ruuskanen J., Cyrys J., Grieken R.V., Hartog J.J., Kreyling W.G., Pekkanen J., 2005. Sources and elemental composition of ambient PM2.5 in three European cities. Sci. Tot. Env. 337, 147–162.

Vecchi R., Marcazzan G., Valli G., 2007. A study on nighttime-daytime PM10 concentration and elemental composition in relation to atmospheric dispersion in the urban area of Milan (Italy), Atmos. Environ., 41, 2136–2144.

Wang X.L., Sato T., Xing B.S., 2006. Size distribution and anthropogenic sources apportionment of airborne trace metals in Kanazawa, Japan. Chemosphere, 65, 2440–2448.

Wedepohl, K.H., 1995. The composition of the continental crust. Geochim. Cosmochim. Acta 59, 1217–1232.

World Health Organization Europe, 2006. Air Quality Guidelines -Global Update 2005. Geneva: World Health Organization.

World Meteorological Organization, 2012. Cold spell in Europe and Asia in late winter 2011/2012. https://www.wmo.int/pages/mediacentre/news/documents/dwd_2012_report.pdf. Accessed 15 February 2015.

Yli-Tuomi, T., Venditte, L.,Hpoke, P.K., Basunia,M.S., Landsberger, S., Viisanen, Y., Paatero, J., 2003. Composition of the Finnish Arctic aerosol: collection and analysis of historic filter samples. Atmos. Environ. 37, 2355–2364.

Table and Figure Captions

Table 1. Daily mean micrometeorological variables during the first sampling period (3-10 October 2011). The weather was characterized by stable atmosphere, clear sky (cloud cover 2/8 on 6 October). Due to high nocturnal RH, in the days 03-06 October during the night and in the morning the visibility was low due to fog formation at ground. On 7 October (hours 96-120) an episode of katabatic wind from W-NW, caused RH and temperature reduction, with a slow rebound in the subsequent days, and a increase in visibility.

Table 2. Daily mean micrometeorological variables during the second sampling period (17-24 January 2012). The weather was characterized by stable atmosphere, clear sky. Fog formation at ground during the first three days. On 20-21 January an episode of Foehn (W-NW) occurred; temperatures, mixing, transport and visibility increased.

Table 3. Daily mean micrometeorological variables during the third sampling period (03-10 February 2012), after snow. The weather was characterized by stable atmosphere, clear sky, except on 07 February. Fog formation at ground.

Table 4. Mean concentrations and standard deviation of NO, NO_2 and O_3 during the three sampling periods. EU limits are reported for comparison (8-hour daily average limit for O_3 (120 μg m^{-3}, corresponding to 56 ppbv), annual average for NO_2 (40 μg m^{-3}, corresponding to 19.5 ppbv)).

Table 5. Mean concentrations and their standard deviation of Hexane, Isooctane, BTEX and selected CFCs during the three sampling periods.

Table 6. Mean concentration in ng m^{-3} measured in the three sampling periods (October 2011, January 2011 and February 2011) in Turin city and mean concentration observed in some Italian and European urban areas.

Figure 1. Size resolved gravimetric distribution of airborne particulate matter sampled in February with a eight stages Andersen MkII nonviable cascade impactor.

Figure 2. Element size distributions during October (A), January (B) and February (C) sampling periods.

Figure 3. Enrichment Factors (EFs) of the elements calculated as average values for three sampling periods considered. Coarse fraction: 2.7 – 11 μm; fine fraction: < 2.7 μm.

Figure 4. Score (a) and loading (b) plot on PC1-PC2 for all sampling periods.

Tables And Figures

Day [dd/mm/yyyy]	Mean Pressure [hPa]	Temperature (T_{min} - T_{max}) [C°]	RH (RH_{min} - RH_{max}) [%]	Mean wind speed (max speed) [m/s]	Max Total solar radiation [W/m^2]	Visibility
03/10/2011	1023	21.4 (16.2 - 27.8)	68 (48 - 86)	1.1 (2.5)	497	Low
04/10/2011	1021	21.6 (16.5 - 28.3)	69 (46 - 88)	1.1 (2.8)	510	Low
05/10/2011	1020	21.2 (16.5 - 27.3)	72 (53 - 85)	1.2 (2.5)	467	Low
06/10/2011	1015	21.3 (17.9 - 25.3)	70 (55 - 85)	1.7 (3.7)	436	Low
07/10/2011	1009	18.9 (12.8 - 22.0)	44 (21 - 87)	3.5 (11.4)	559	Good
08/10/2011	1012	15.4 (8.9 - 21.3)	44 (31 - 66)	2.8 (9.8)	583	Good
09/10/2011	1017	14.0 (8.4 - 20.8)	55 (36 - 79)	1.2 (3.7)	519	Good
10/10/2011	1020	15.1 (9.2 - 22.4)	57 (37 - 78)	1.4 (3.2)	541	Good

Table 1. Daily mean micrometeorological variables during the first sampling period (3-10 october 2011). The weather was characterized by stable atmosphere, clear sky (cloud cover 2/8 on 6 october). Due to high nocturnal RH, in the days 03-06 october during the night and in the morning the visibility was low due to fog formation at ground. On 7 october (hours 96-120) an episode of katabatic wind from W-NW, caused RH and temperature reduction, with a slow rebound in the subsequent days, and a increase in visibility.

Day [dd/mm/yyyy]	Mean Pressure [hPa]	Temperature (T_{min} - T_{max}) [C°]	RH (RH_{min} - RH_{max}) [%]	Mean wind speed (max speed) [m/s]	Max Total solar radiation [W/m^2]	Visibility
17/01/12	1026	-0.5 (-4.3 – 5.5)	81 (61 - 87)	0.8 (2.3)	371	Low
18/01/12	1030	-0.5 (-4.2 – 4.4)	80 (46 - 88)	0.8 (2.0)	295	Low
19/01/12	1026	0.6 (-3.0 – 4.6)	76 (65 - 83)	0.6 (2.3)	219	Low
20/01/12	1014	7.9 (-0.9 – 17.0)	55 (30 - 86)	4.1 (11.0)	386	Good
21/01/12	1013	8.3 (3.9 – 13.4)	57 (37 - 82)	1.7 (11.4)	298	Good
22/01/12	1009	7.8 (2.7 - 15.3)	70 (46 - 86)	0.9 (3.8)	352	Good
23/01/12	1012	5.3 (2.6 – 10.6)	82 (63 - 89)	0.9 (3.0)	282	Good
24/01/12	1014	4.8 (1.9 – 11.8)	79 (53 - 89)	1.0 (12.5)	355	Good

Table 2. Daily mean micrometeorological variables during the second sampling period (17-24 January 2012). The weather was characterized by stable atmosphere, clear sky. Fog formation at ground during the first three days. On 20-21 January an episode of Foehn (W-NW) occurred; temperatures, mixing, transport and visibility increased.

Day [dd/mm/yyyy]	Mean Pressure [hPa]	Temperature (T_{min} - T_{max}) [C°]	RH (RH_{min} - RH_{max}) [%]	Mean wind speed (max speed) [m/s]	Max Total solar radiation [W/m^2]	Visibility
03/02/2012	1018	-2.5 (-5.1 – 0.0)	72 (56 - 82)	0.7 (3.2)	408	Low
04/02/2012	1019	-4.6 (-8.0 – -1.1)	72 (60 - 82)	0.9 (2.4)	232	Low
05/02/2012	1022	-4.8 (-8.6 – 0.0)	72 (59 - 82)	1.0 (2.5)	418	Low
06/02/2012	1017	-6.8 (-12.3 – -0.1)	73 (52 - 83)	1.1 (4.5)	516	Low
07/02/2012	1014	-5.2 (-12.5 – -0.8)	71 (55 - 84)	1.1 (5.0)	329	Low
08/02/2012	1024	1.1 (-1.8 – 4.8)	70 (48 - 87)	0.8 (3.2)	427	Low
09/02/2012	1019	-1.7 (-7.2 – 2.5)	76 (59 - 86)	0.8 (3.0)	486	Low
10/02/2012	1021	-1.9 (-3.6 – -0.2)	72 (48 - 85)	1.3 (4.1)	399	Low

Table 3. Daily mean micrometeorological variables during the third sampling period (03-10 February 2012), after snow. The weather was characterized by stable atmosphere, clear sky, except on 07 February. Fog formation at ground.

	Mean Concentrations and their Standard Deviation over the entire sampling periods, ppbv			EU Limits, ppbv
	October	January	February	
NO	10.1 ± 16.3	87.3 ± 63.5	49.5 ± 42.2	
NO_2	22.9 ± 14.7	40.5 ± 15.3	48.5 ± 12.5	19.5
O_3	19.3 ± 15.9	3.3 ± 5.2	5.7 ± 7.1	56.0

Table 4. Mean concentrations and their standard deviations of NO, NO_2 and O_3 during the three sampling periods. EU limits are reported for comparison (8-hour daily average limit for O_3 (120 µg m^{-3}, corresponding to 56 ppbv), annual average for NO_2 (40 µg m^{-3}, corresponding to 19.5 ppbv))

	Mean Concentrations and their Standard Deviations over the entire sampling periods, ppbv		
	October	**January**	**February**
Hexane	0.24 ± 0.15	0.24 ± 0.20	0.08 ± 0.04
Isooctane	0.12 ± 0.10	0.12 ± 0.09	0.05 ± 0.05
Benzene	0.72 ± 0.57	2.20 ± 1.49	1.15 ± 0.55
Toluene	2.50 ± 2.04	3.42 ± 2.50	1.44 ± 0.87
Ethylbenzene	0.20 ± 0.16	0.30 ± 0.27	0.11 ± 0.08
m and p-Xylene	0.56 ± 0.47	0.81 ± 0.24	0.30 ± 0.29
o-Xylene	0.26 ± 0.22	0.35 ± 0.31	0.12 ± 0.09
CFC12	0.62 ± 0.09	0.60 ± 0.03	0.59 ± 0.05
CFC11	0.29 ± 0.04	0.30 ± 0.02	0.27 ± 0.01
CFC113	0.09 ± 0.005	0.09 ± 0.003	0.09 ± 0.004

Table 5. Mean concentrations and their standard deviations of Hexane, Isooctane, BTEX and selected CFCs during the three sampling periods.

	As	Co	Cd	Cr	Cu	Fe	Mn	Mo	Ni	Pb	Pd	Pt	Rh	Sn	V	Zn
October	0.05	0.02	1.85	0.83	2.44	105	2.50	0.28	1.17	1.53	0.03	0.03	0.003	30.2	0.08	32.7
January	0.03	0.04	0.35	0.73	1.88	207	3.10	0.22	1.05	1.88	0.03	0.02	0.016	5.32	0.30	17.8
February	0.13	0.06	0.80	0.54	2.52	110	2.22	0.34	1.55	2.25	0.02	0.02	0.007	7.82	0.27	21.0
Milan[a]	-	-	-	13	72	1830	45		10	71						180
Palermo[b]	1.5	0.3		6.5	49	496	12	3.9	5.5	18					20	48
Rome[c]												0.02	0.004			
Venice[d]	3		1.9		8	247	14		6	16					6	47
Stockholm[e]	0.88	0.15	0.11	2.3	7.7		5.5	1.6	2.3	3.4				14	1.6	17
Edinburgh[f]	0.37		0.34	1.60	4.93	183	2.94		3.43	14.1					1.14	13.3
Barcelona[g]				6.0	74		24		7.0	149					13	250

[a] Vecchi et al. (2007).
[b] Dongarrà et al. (2007).
[c] Bocca et al. (2003)
[d] Toscano et al. (2011).
[e] Johansson et al. (2009).
[f] Heal et al. (2005).
[g] Querol et al. (2001).

Table 6. Mean concentration in ng m^{-3} measured in the three sampling periods (October 2011, January 2011 and February 2011) in Turin city and mean concentration observed in some Italian and European urban areas.

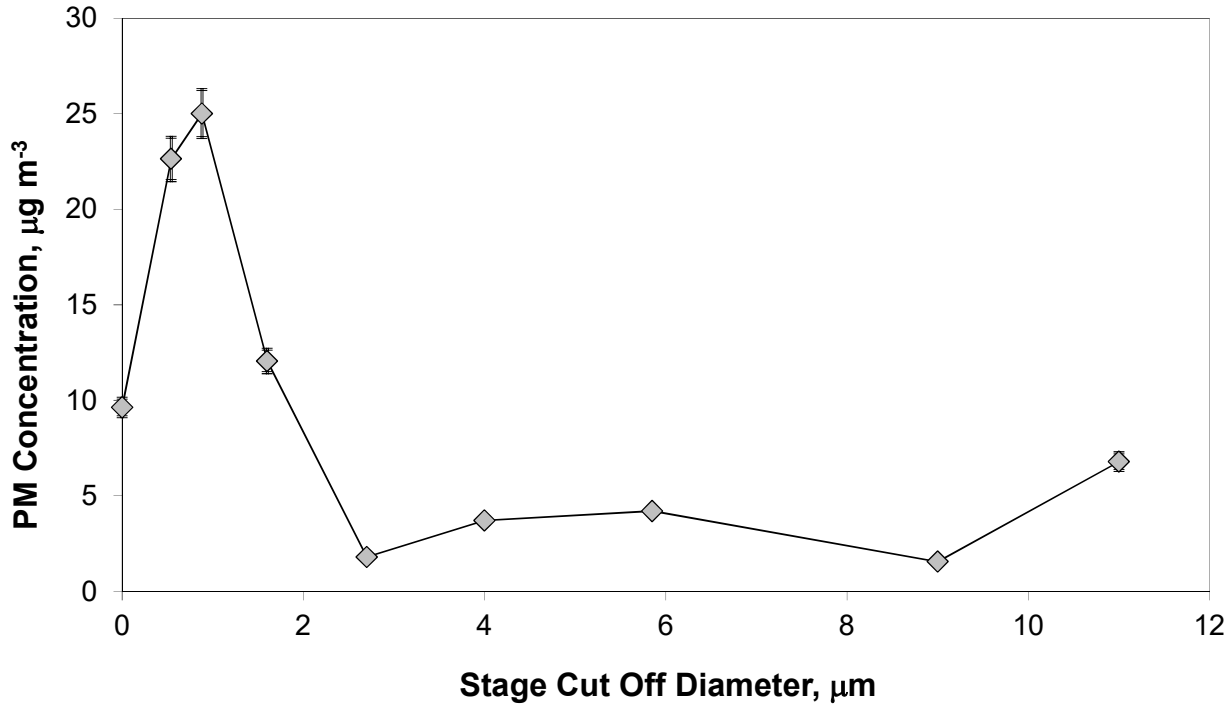

Figure 1. Size resolved gravimetric distribution of airborne particulate matter sampled in February with a eight stages Andersen MkII nonviable cascade impactor.

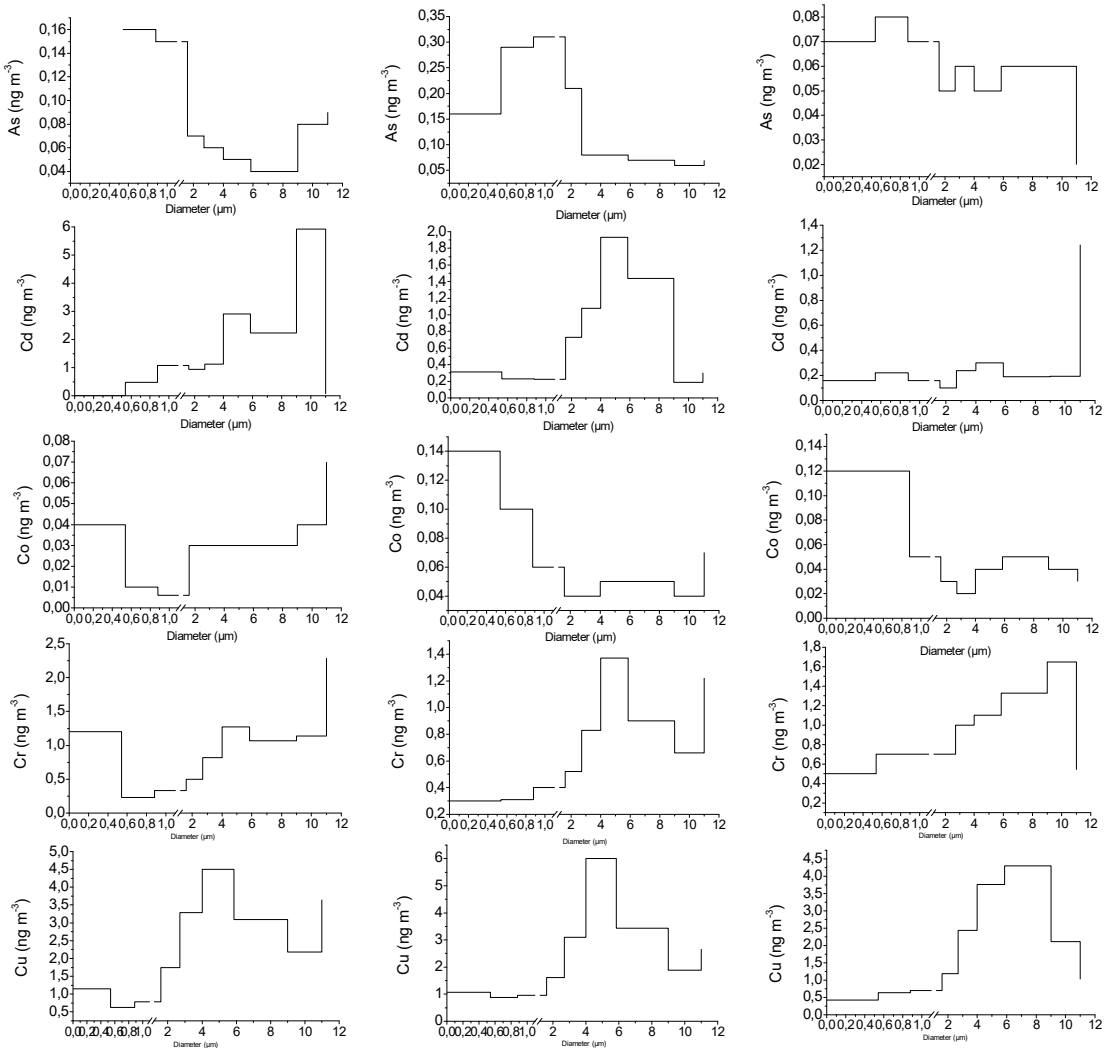

Figure 2A

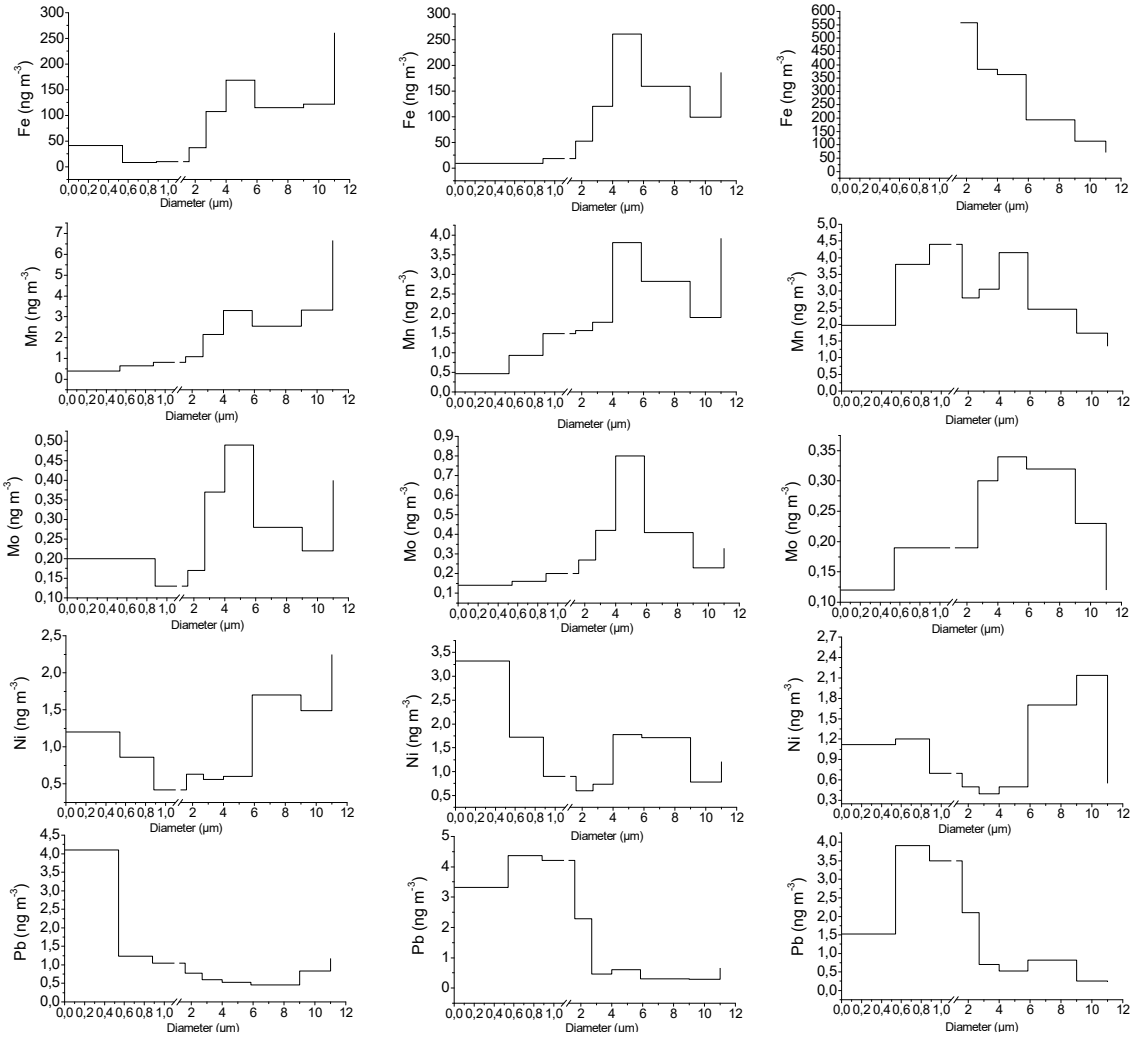

Figure 2B

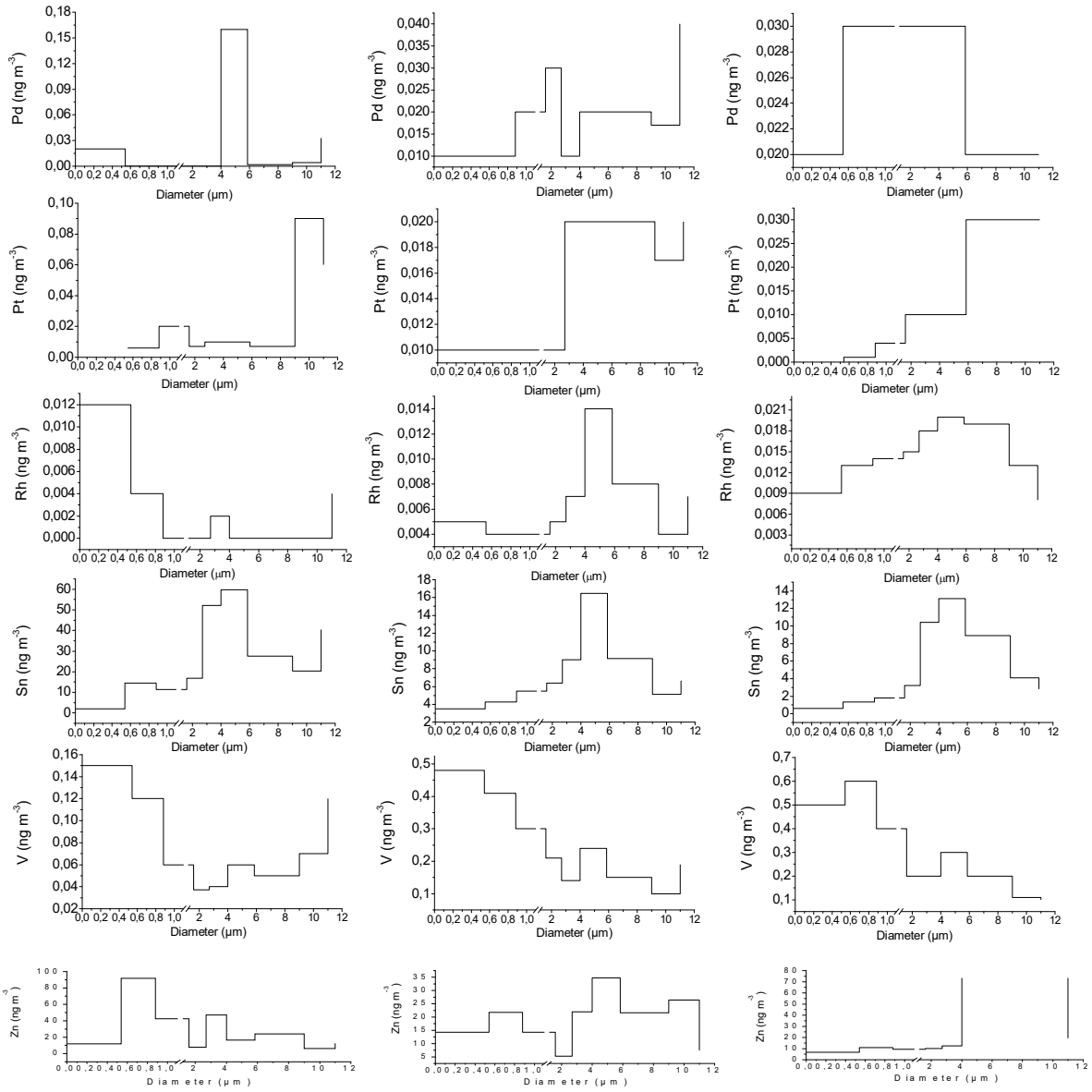

Figure 2C

Figure 2. Element size distributions during October (A), January (B) and February (C) sampling periods.

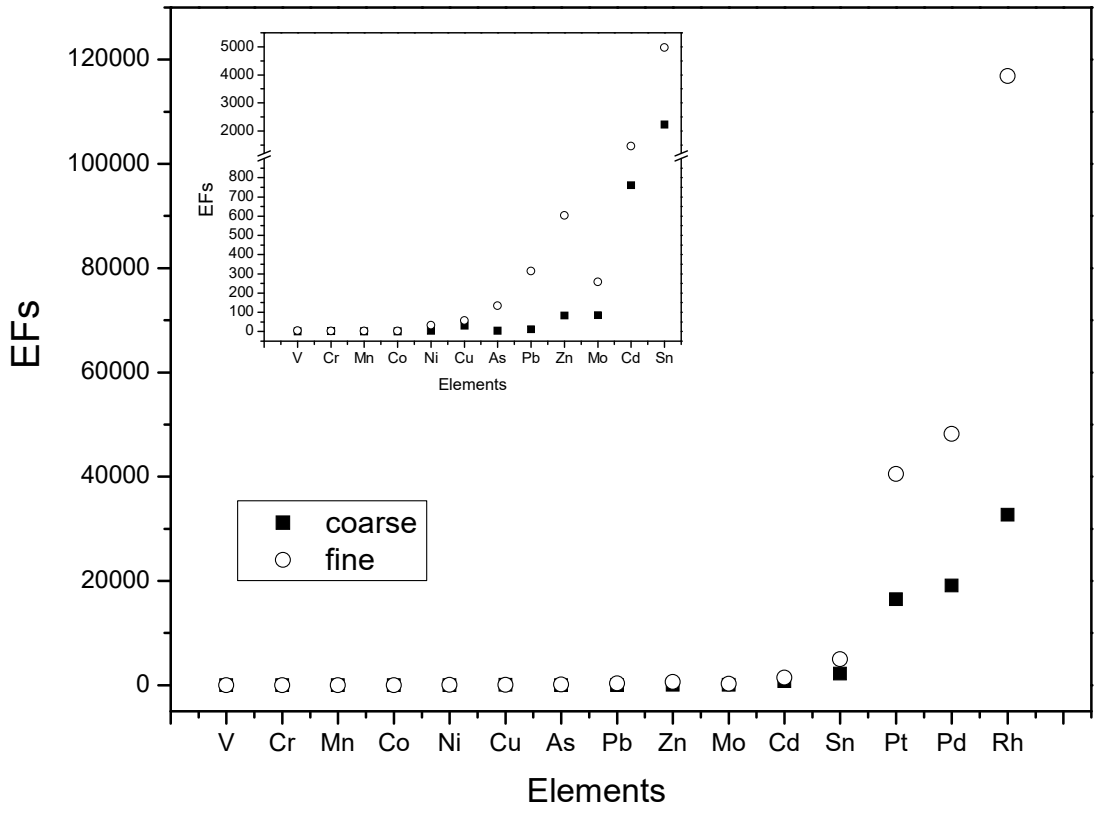

Figure 3. Enrichment Factors (EFs) of the elements calculated as average values for three sampling periods considered. Coarse fraction: 2.7 – 11 µm; fine fraction: < 2.7 µm.

a)

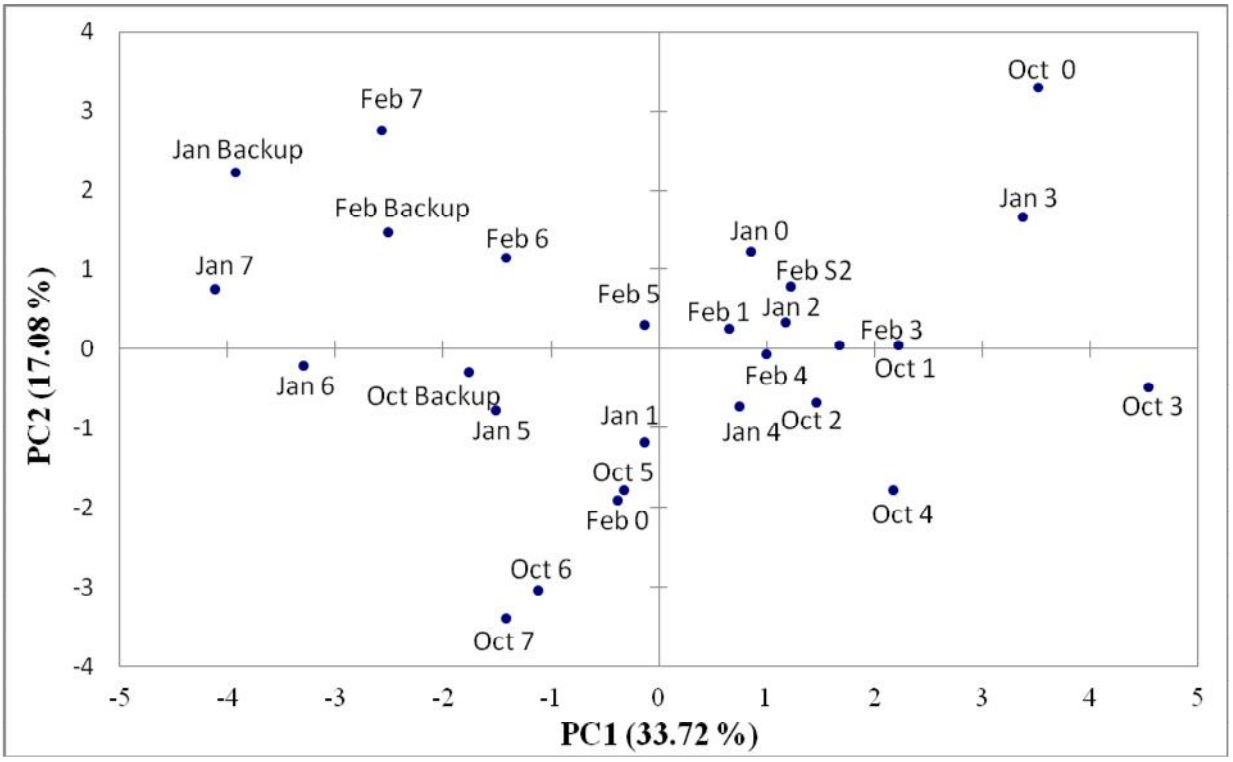

b)

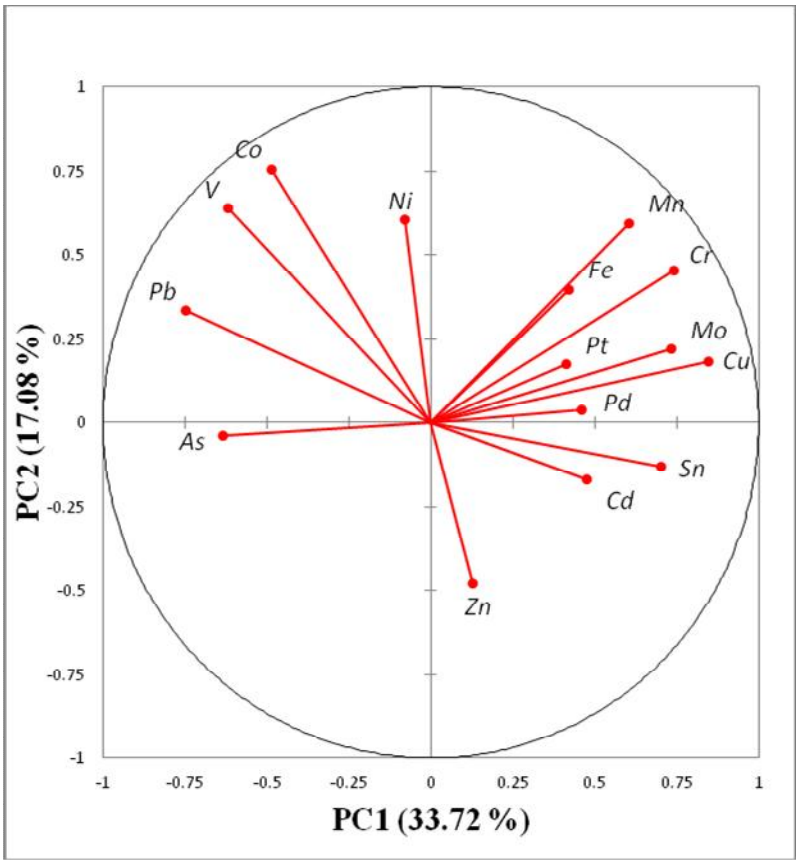

Figure 4. Score (a) and loading (b) plot on PC1-PC2 for all sampling periods.